



# Obesity-Associated Conditions Hinder Solute Drainage Function of Engineered Human Lymphatic Vessels

Alex J. Seibel<sup>1</sup> · Cheyanne L. Frosti<sup>2</sup> · Abderrahman R. Tlemçani<sup>1</sup> · Nikhil Lahiri<sup>1</sup> · Joely A. Brammer-DePuy<sup>1</sup> · Matthew D. Layne<sup>2</sup> · Joe Tien<sup>1,3</sup>

Received: 2 August 2024 / Accepted: 13 December 2024 / Published online: 23 January 2025  
© The Author(s), under exclusive licence to Biomedical Engineering Society 2025

## Abstract

**Purpose** Obesity is associated with poor lymphatic solute drainage. It is unclear whether the chronic inflammation, hypoxia, and hyperlipidemia that are together associated with obesity cause impaired drainage function, and if so, whether these conditions act directly on lymphatic endothelial cells (LECs) or are indirectly mediated by the mechanical properties or cellular composition of the surrounding tissue.

**Methods** We engineered blind-ended lymphatic vessels in type I collagen gels and simulated the obese microenvironment with a cocktail of tumor necrosis factor (TNF)- $\alpha$ , cobalt chloride (CoCl<sub>2</sub>), and oleate, which model inflammation, hypoxia, and hyperlipidemia, respectively. We compared the solute drainage rate and leakage of lymphatics that were exposed to simulated obesity or not. We performed similar assays with lymphatics in stiffened gels, in adipocyte-laden gels, or in the presence of conditioned medium (CM) from adipose cells treated with the same cocktail.

**Results** Lymphatics that were exposed to simulated obesity exhibited more gaps in endothelial junctions, leaked more solute, and drained solute less quickly than control lymphatics did, regardless of matrix stiffness. CM from adipose cells that were exposed to simulated obesity did not affect lymphatics. Lymphatics in adipocyte-laden gels did not exhibit worse drainage function when exposed to simulated obesity.

**Conclusions** The combination of obesity-associated inflammation, hypoxia, and hyperlipidemia impairs lymphatic solute drainage and does so by acting directly on LECs. Surprisingly, adipocytes may play a protective role in preventing obesity-associated conditions from impairing lymphatic solute drainage.

**Keywords** Lymphoscintigraphy · Microfluidics · Microphysiological system · Microvascular tissue engineering · Vascular physiology

## Abbreviations

CM Conditioned medium  
DM Differentiation medium

LEC Lymphatic endothelial cell  
LM Lymphatic medium

## Introduction

Obesity is an important risk factor for lymphatic dysfunction [1, 2]. For instance, a body mass index (BMI) greater than 50–55 can lead to lymphedema with no known precipitating event [3]. Moreover, in cancer patients, obesity increases the risk of developing lymphedema secondary to removal of lymph nodes [4]. Initially, it was hypothesized that the hypertrophic adipose tissue in obesity can compress lymphatic vessels and generate excess interstitial fluid, thereby overwhelming the ability of those vessels to drain the fluid [3]. This explanation is incomplete, however, since weight loss does not fully reverse lymphedema [5].

Associate Editor Michael R. King oversaw the review of this article.

✉ Joe Tien  
jtien@bu.edu

<sup>1</sup> Department of Biomedical Engineering, Boston University, 44 Cummington Mall, Boston, MA 02215, USA

<sup>2</sup> Department of Biochemistry & Cell Biology, Boston University Chobanian & Avedisian School of Medicine, Boston, MA, USA

<sup>3</sup> Division of Materials Science and Engineering, Boston University, Boston, MA, USA

It is likely that obesity-related changes other than enlargement of adipose tissue per se can adversely affect lymphatic function. For example, obesity-associated fibrosis often persists after weight loss [6] and could contribute to lymphatic dysfunction.

Obesity is now accepted to cause microenvironmental changes in adipose tissue that result in inflammation, hypoxia, and fibrosis [7, 8]. In obese individuals, adipose tissue is hypovascular [9], which causes the development of hypoxia, the recruitment of macrophages, and the development of low-level chronic inflammation and fibrosis [10, 11]. The adipose tissue in obesity has elevated tumor necrosis factor (TNF)- $\alpha$  levels that correlate with insulin resistance [12]. Obesity is also associated with an increased rate of lipolysis in adipocytes, which is accompanied by elevated local and/or circulating levels of free fatty acids (FFAs) [13, 14].

The effects of obesity-associated microenvironmental changes on lymphatic function, especially solute drainage, remain poorly understood. The collecting lymphatics of obese mice exhibit reduced pumping, in part from obesity-associated perilymphatic inflammation and nitric oxide production [15]. Mesenteric lymphatics in obese mice and humans are leaky via cyclooxygenase and vascular endothelial growth factor (VEGF)-C signaling [16], while lymphatic dysfunction in other vascular beds remain less well-studied.

The main goal of our study is to determine, using an engineered 3D model, whether the combination of inflammatory factors, hypoxia, and FFAs that characterizes obesity can impair lymphatic solute drainage function. The ability of these factors, when presented individually, to disrupt lymphatic endothelial junctions, promote lymphangiogenesis, and/or inhibit lymphatic contractility supports the possibility that these factors together could affect solute drainage [17–21]. A second goal of this work is to determine whether other elements of the obese tissue environment, such as matrix stiffness (secondary to fibrosis) and the presence of adipocytes, may modify any alteration of lymphatic drainage function.

To this end, we engineered 3D *in vitro* models of lymphatic vessels, subjected them to a combination of obesity-associated conditions—chronic inflammation, hypoxia, and tissue hyperlipidemia—and measured their drainage function. Inflammation, hypoxia, and hyperlipidemia were simulated *in vitro* by exposure to TNF- $\alpha$ , cobalt chloride (CoCl<sub>2</sub>), and oleic acid, respectively. We found that this “simulated obesity” impaired solute drainage of the lymphatic vessels in both soft and stiff collagen gels, most likely via disruption of lymphatic junctions. In contrast, simulated obesity did not affect lymphatic solute drainage or lymphatic junctions in adipocyte-laden gels. Conditioned medium from adipose cells that were exposed to the same obesity-associated conditions also had no effect on drainage function of lymphatics.

Thus, obesity-associated inflammation, hypoxia, and hyperlipidemia together decrease lymphatic drainage function via a direct effect on lymphatic endothelium.

## Materials and Methods

### Cell Culture

Human dermal lymphatic microvascular endothelial cells (LECs, lots #2011204 and #0070602 from male donors; Promocell) were cultured on gelatin-coated tissue culture plates in lymphatic medium (LM) that consisted of MCDB131 (Caisson) supplemented with 10% heat-inactivated fetal bovine serum (FBS, lot #G20106; Bio-Techne), 1% glutamine-penicillin-streptomycin (GPS; Invitrogen), 1  $\mu$ g/mL hydrocortisone (Sigma), 80  $\mu$ M dibutyryl cyclic AMP (dbcAMP; Sigma), 25  $\mu$ g/mL endothelial cell growth supplement (Alfa Aesar), 2 U/mL heparin (Sigma), and 0.2 mM ascorbic acid 2-phosphate (Sigma). LECs were passaged every 2–3 days at a 1:4 ratio through passage eight using 0.005% trypsin.

Telomerase-immortalized human adipose-derived stem cells (ASCs) from white adipose tissue [22] were cultured in high-glucose DMEM (Gibco) supplemented with 10% FBS and 1% GPS. Although immortalized, these cells accumulate lipid and express similar levels of adipogenic markers compared to their parental primary cells after standard adipogenic differentiation [22]. ASCs were passaged every three days at a 1:4 ratio using 0.25% trypsin.

Confluent dishes of ASCs were differentiated into adipocytes using differentiation medium (DM) that consisted of high-glucose DMEM supplemented with 2% FBS, 1% GPS, 0.1  $\mu$ M dexamethasone (Sigma), 0.5  $\mu$ M bovine insulin (Sigma), 500  $\mu$ M 1-methyl-3-isobutylxanthine (Sigma), 30  $\mu$ M indomethacin (Sigma), 2 nM triiodo-L-thyronine (Sigma), 17  $\mu$ M pantothenate (Sigma), and 33  $\mu$ M D-biotin (Sigma). Medium was replaced every three days. Nine days after the start of differentiation, medium was supplemented with 0.4 mM sodium oleate (Sigma) and 1% lipid-poor bovine serum albumin (BSA; Calbiochem) to accelerate the accumulation of lipid. Cells were differentiated for 2.5–4 weeks (i.e., 9–21 days of treatment with oleate) before use. On average,  $56.1 \pm 3.7\%$  of the cultured ASCs differentiated into adipocytes, as assessed by staining with Nile Red. We refer to DM-treated cultures, which contain adipocytes and residual non-adipocytes, as “adipose cells”.

### Collection of Conditioned Medium

Adipose cell-conditioned medium was obtained by adding DM (10 mL per 100-mm-diameter dish) to adipose cells for one day at 37 °C, collecting the medium, and freezing the

medium at  $-80^{\circ}\text{C}$ . Medium was thawed and sterile-filtered ( $0.2\ \mu\text{m}$ ; Corning) before use.

### Formation of Patterned Collagen Gels

Blind-ended cavities were formed in type I collagen gels using a previously described technique (Fig. 1) [23, 24]. Briefly, polydimethylsiloxane (PDMS) chambers that contained 18-mm-long channels with  $1\ \text{mm} \times 1\ \text{mm}$  cross-sections were UV/ozone-treated and placed feature-side down onto glass coverslips. The channels were coated with poly-D-lysine (300 kDa, 1 mg/mL in PBS; Sigma). Acupuncture needles (120  $\mu\text{m}$  in diameter; Seirin) were brushed gently over a laboratory bench to round the tips, coated with BSA (1% in PBS), and aligned inside the chambers so that the

tips of the needles were located 1–1.5 mm from the end of the channels.

A neutralized solution of type I collagen (7 mg/mL, pH 7–7.5, from rat tail; Corning) was used to prepare three gel compositions: (i) *Uncrosslinked adipocyte-free gels*: The collagen mixture consisted of 100  $\mu\text{L}$  of neutralized collagen and 4  $\mu\text{L}$  of DM to obtain a final collagen concentration of 6.7 mg/mL. (ii) *Crosslinked adipocyte-free gels*: The original 7 mg/mL solution of neutralized collagen was used. (iii) *Uncrosslinked adipocyte-laden gels*: We washed cultures of adipose cells twice with PBS and treated the cultures for 10 min with a 1:1 mixture of collagenase (1 mg/mL in HBSS; Worthington Biochemical) and 0.25% trypsin. Cells were collected in DM and centrifuged at 500 g for 5 min. Residual collagenase was removed by washing the cells once with DM, and cells were centrifuged once more. After centrifugation, 4  $\mu\text{L}$  of the floating, adipocyte-rich cell “cake” was added per 100  $\mu\text{L}$  of neutralized collagen. The estimated concentration of adipocytes in the collagen was  $177 \pm 29$  cells/ $\mu\text{L}$ .

For all three types of gel, the collagen mixtures were added around the needles in the channels of the PDMS chambers and polymerized at  $24^{\circ}\text{C}$  for 30 min. Immediately after polymerization, uncrosslinked gels with or without embedded adipocytes (i.e., for gel compositions (i) and (iii)) were hydrated with sample medium. Sample medium for these gels consisted of LM supplemented with 3% 60–90 kDa dextran (MP Biomedicals), 400  $\mu\text{M}$  db-cAMP (final concentration), and 0.5  $\mu\text{M}$  bovine insulin to support vascular stability and to inhibit adipocyte lipolysis and/or dedifferentiation [25–27]. Needles were removed to generate empty, blind-ended cavities in the collagen gels. To promote the flow of medium, we subjected each gel to a slight hydrostatic pressure difference ( $\sim 0.2\ \text{cm H}_2\text{O}$ ) by transferring 20  $\mu\text{L}$  of sample medium from one well to the other.

For gel composition (ii), the adipocyte-free gels were hydrated with PBS following polymerization and removal of needles, and then crosslinked by flushing with 20 mM genipin (Wako Biosciences) in PBS for two hours at  $24^{\circ}\text{C}$ . These crosslinked gels were washed exhaustively with PBS for at least one day to remove residual genipin before washing with sample medium. The sample medium consisted of LM supplemented with 3% dextran and 400  $\mu\text{M}$  db-cAMP (final concentration) to support vascular stability; insulin was not added to the medium. For crosslinked gels that were used in experiments with conditioned medium, the sample medium consisted of a 1:1 mixture of LM and unconditioned DM with final concentrations of 3% dextran and 200  $\mu\text{M}$  db-cAMP, and unconditioned medium was replaced with conditioned medium on day 5.

To prepare gels for seeding of LECs, we conditioned them with sample medium for at least one day.

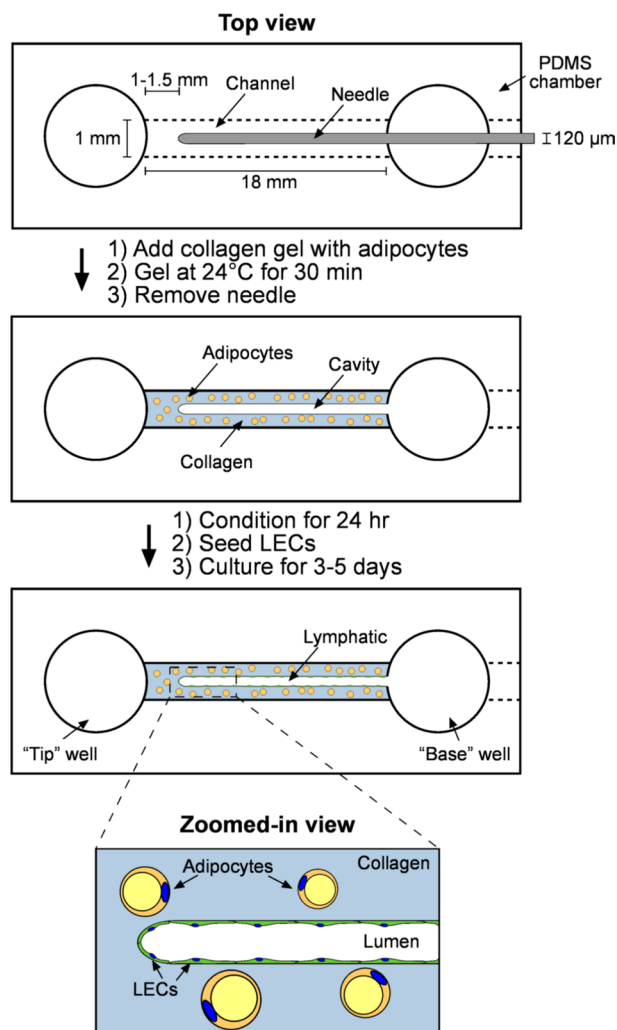
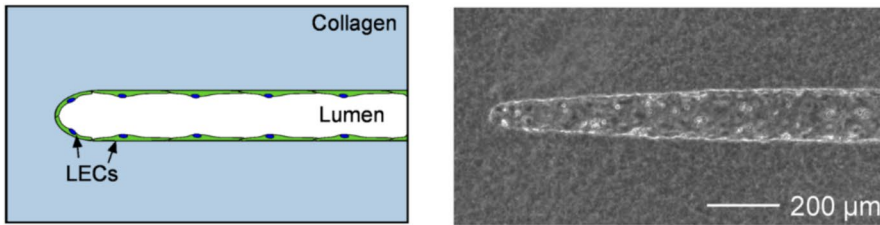


**Fig. 1** Schematic diagram of the engineering of a blind-ended human lymphatic vessel in an adipocyte-laden collagen matrix. A similar procedure with adipocyte-free collagen gel (with or without crosslinker) yielded a human lymphatic model without surrounding adipocytes

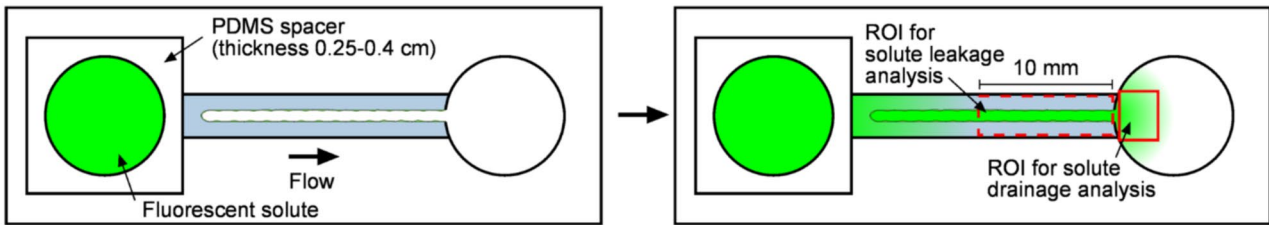
### A Uncrosslinked adipocyte-free collagen



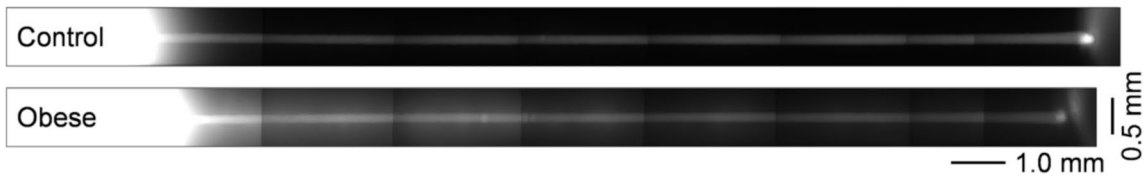
### B

- 1) Add PDMS spacer to tip well
- 2) Fill spacer with medium
- 3) Wait 4 hr, then add fluorescent medium

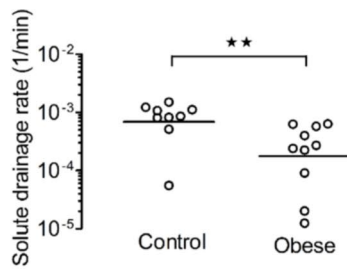
- 1) Flow fluorescent medium for 90 min
- 2) Track solute drainage every 2 min in ROI in base well
- 3) Track solute leakage after 90 min in ROI in gel



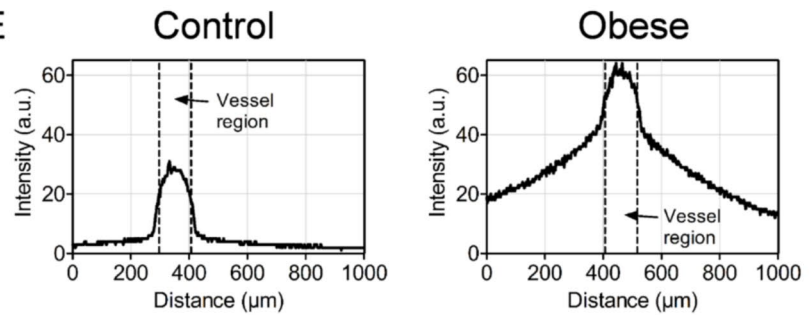
### C



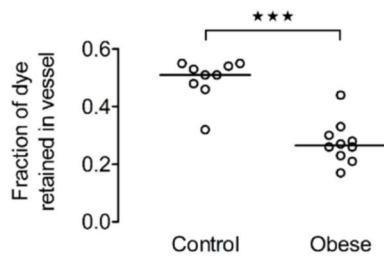
### D



### E



### F



### G

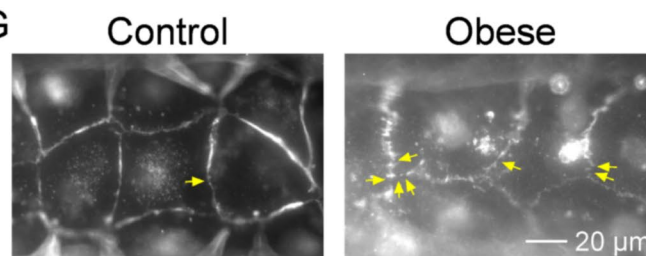


**Fig. 2** Simulated obesity impairs lymphatic solute drainage in uncrosslinked adipocyte-free gels. **A** Schematic (*left*) and phase-contrast image (*right*) of a lymphatic vessel in an uncrosslinked collagen gel on day 3. **B** Schematic of solute drainage assay. **C** Whole-vessel fluorescence images taken 90 min after introduction of solute. Flow is from left to right. **D** Solute drainage rates. **E** Representative traces of the transverse fluorescence intensity profile in control and obesity-treated samples, taken 1 cm from the open end of the vessel. **F** Solute retention fractions. Data in (**D**) and (**F**) are from six independent experiments. **G** Fluorescence images of lymphatic vessels stained for PECAM-1 on day 6 after three days of control treatment or simulated obesity. Images were taken at the bottom surface of the vessel near the vessel tip. Arrows indicate gaps in junctions. \*\*,  $p < 0.01$ ; \*\*\*,  $p < 0.001$

### Formation of Blind-Ended Human Lymphatic Vessels

A total of 125 blind-ended lymphatic vessels were formed in this study using previously described methods [23]: 25 in uncrosslinked, adipocyte-free gels; 54 in crosslinked, adipocyte-free gels; and 46 in uncrosslinked, adipocyte-laden gels. LECs were collected as a dense suspension ( $\sim 10^7$  cells/mL) in sample medium. Cells were seeded into the empty cavities by adding  $\sim 5$   $\mu$ L of cell suspension to the well adjacent to the open end of the cavity (i.e., the “base well”) and  $\sim 3$   $\mu$ L of cell-free sample medium to the well adjacent to the tip of the cavity (i.e., the “tip well”), which allowed hydrostatic pressure to advect cells into the cavities. Once the LECs reached the tips of the cavities, 5–10  $\mu$ L of sample medium was added to the tip wells to prevent more cells from entering the cavities. After 15 min,  $\sim 50$   $\mu$ L of sample medium was added to the tip wells to flow any non-adherent LECs out of the cavities. The base wells were rinsed three times with sample medium to remove non-adherent cells. Samples were then refed twice a day for at least three days by adding 75  $\mu$ L of sample medium to the base wells and 25  $\mu$ L of sample medium to the tip wells. Only vessels that reached confluency in 3–5 days were kept for experiments.

### Simulation of Obesity-Associated Conditions

To simulate obesity and produce “obesity-treated” lymphatics, we added 10 ng/mL TNF- $\alpha$ , 50  $\mu$ M CoCl<sub>2</sub>, and 0.4 mM oleic acid (with 1% BSA as a carrier) in sample medium to lymphatics on day 3 (i.e., three days after the seeding of LECs) and continued treatment for three days. These concentrations were chosen from published studies [17, 19, 28, 29]. We also added this cocktail to adipose cells in DM in 2D culture for three days to produce “obesity-treated” adipose cells. For some experiments, CM (“obesity-treated CM”) was collected from these adipose cells and added to lymphatics for three days starting on day 5.

### Characterization of Embedded Adipocytes

The viability of embedded cells in the adipose/lymphatic co-culture model was tested on day 3 by supplementing the medium with propidium iodide (PI, 2  $\mu$ g/mL; Invitrogen) and Hoechst 33342 (10  $\mu$ g/mL; Invitrogen) for 30 min. Samples were imaged near the tip of the vessel using a 1 mm  $\times$  1.4 mm field of view. Viability is reported as the percentage of embedded cells that were PI-negative.

The percentage of embedded cells that remained adipocytes on day 3 was measured in fixed samples (fixation is detailed below in “Immunofluorescence staining”) based on the morphology and lipid content of the cells. Circularity ( $C$ ) of a cell was calculated as  $C = 4\pi A/P^2$ , where  $A$  and  $P$  are the area and perimeter of the cell, respectively. A circularity of 1 represents a perfect circle, and a circularity of 0 represents a curve with no enclosed area. Cells with a circularity of at least 0.65 were considered round; otherwise, they were considered elongated. Adipocytes were defined as round cells that were Nile Red-positive. Dedifferentiated cells were defined as elongated cells that were Nile Red-negative. Round, Nile Red-negative cells and elongated, Nile Red-positive cells were considered to be partially dedifferentiated. Adipocyte diameter was defined as the maximum width of an adipocyte.

### Solute Drainage Assay

Following a previous protocol [24], we measured the ability of lymphatics to drain solute after three days of treatment (i.e., on day 6 for obesity-treated lymphatics or on day 8 for lymphatics cultured with obesity-treated CM from adipose cells). We first placed vessels under a drainage-promoting pressure difference of 0.25 cm H<sub>2</sub>O (for samples with 6.7 mg/mL collagen gels) or 0.4 cm H<sub>2</sub>O (for samples with 7.0 mg/mL collagen gels) by adding a PDMS spacer and additional medium to the tip well of the sample. Under these conditions, the pressure at the blind end of the lymphatic was greater than the pressure at the open end. After four hours, medium in the tip well was replaced with medium that contained 100  $\mu$ g/mL Alexa Fluor 488-or 594-conjugated dextran (10 kDa; Invitrogen). Alexa Fluor 594 was used for Figs. 2 and 7; Alexa Fluor 488 was used instead for Figs. 3 and 5 to avoid autofluorescence from crosslinked gels. A rectangular region of interest (ROI) adjacent to the open end of the vessel was then imaged every two minutes for ninety minutes with a Plan-Neofluar 5  $\times$  0.15 NA objective (Zeiss) to track fluorescence intensity. All samples were imaged with identical microscope settings, and exposure times were chosen so that fluorescence detection was within the linear range and not saturated. Images were corrected for non-uniform illumination using Axiovision ver. 4.5. Solute drainage rates

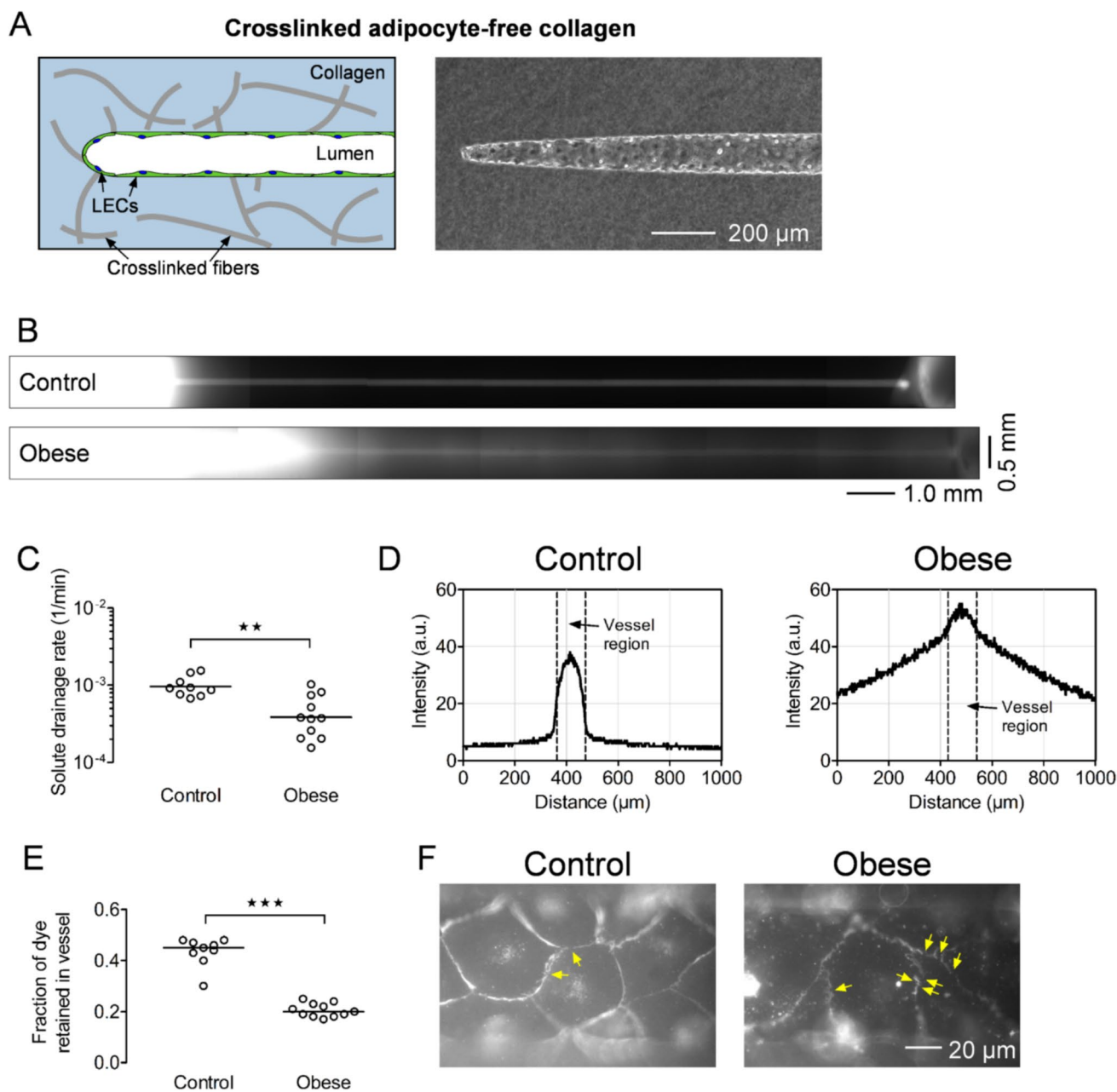


**Fig. 3** Simulated obesity impairs lymphatic solute drainage in crosslinked adipocyte-free gels. **A** Schematic (*left*) and phase-contrast image (*right*) of a lymphatic vessel in a crosslinked gel on day 3. **B** Whole-vessel fluorescence images taken 90 min after introduction of solute. Flow is from left to right. **C** Solute drainage rates. **D** Representative traces of the transverse fluorescence intensity profile, taken

1 cm from the open end of the vessel. **E** Solute retention fractions. Data in (**C**) and (**E**) are from six independent experiments. **F** Fluorescence images of lymphatic vessels stained for PECAM-1 on day 6 after three days of control treatment or simulated obesity. Images were taken at the bottom surface of the vessel near the vessel tip. Arrows indicate gaps in junctions. \*\*,  $p < 0.01$ ; \*\*\*,  $p < 0.001$

(equivalent to lymphoscintigraphy rate constants [30]) were calculated as described previously using ImageJ [24]. Once time-lapse imaging of the ROI was complete (i.e., after 90 min of drainage), a composite fluorescence image of the whole vessel was obtained by stitching overlapping images. Solute leakage at 90 min was determined from

the composite image using ImageJ by examining the final 1 cm of the sample closest to the open end of the vessel, subtracting background fluorescence, and calculating the ratio of integrated fluorescence signal solely within the vessel lumen over the signal in the vessel plus surrounding matrix.

## Immunofluorescence Staining

Lymphatic vessels in cell-free and in adipocyte-containing gels were fixed before (on day 3 or 5) or after (on day 6 or 8) obesity treatment and stained as described previously [31, 32]. Briefly, samples were fixed in 4% paraformaldehyde (PFA; Electron Microscopy Sciences) for 15 min at room temperature and washed with PBS. Samples were then removed from the PDMS chambers, placed into PBS in microcentrifuge tubes, and stored at 4 °C until use. Samples were permeabilized with 0.2% Triton X-100 (Sigma) in PBS (i.e., PBST) for 30 min and treated with blocking buffer that consisted of 5% goat serum (GS; Invitrogen) in PBST for 4 hr at room temperature. Primary antibodies were prepared in blocking buffer, applied to the samples overnight at 4 °C, and washed out by transferring samples to fresh tubes with PBST. Sequential washes were performed at least six times for 30 min each on a rocker at room temperature. An identical protocol was followed to apply secondary antibodies, Hoechst 33342 (10 µg/mL), and Nile Red (1 µg/mL; Sigma). Primary antibodies and their working concentrations were mouse anti-PECAM-1 (clone WM-59, 10 µg/mL; Sigma), rabbit anti-Prox1 (1:1000, absolute concentration unknown; Upstate), mouse anti-VE-cadherin (clone 75, 2.5 µg/mL; BD Transduction Laboratories), and rabbit anti-perilipin 1 (5 µg/mL; Invitrogen). Secondary antibodies were highly cross-adsorbed Alexa Fluor 488- or 594-conjugated goat anti-mouse IgG and anti-rabbit IgG (5 µg/mL; Invitrogen).

Cultures of LECs, undifferentiated ASCs, and adipose cells were also grown on coverslips, fixed, and stained for Prox1. The LECs and undifferentiated ASCs served as the positive and negative controls, respectively. Before fixing, the adipose cells were exposed to lymphatic sample medium with insulin for three days to approximate the conditions of the embedded adipocytes in the 3D adipose/lymphatic coculture model. Cells were fixed with 4% PFA, washed with PBS, and treated with blocking buffer for 30 min. Primary antibody was applied for 1 hr at room temperature, and cells were washed three times with blocking buffer for 5 min each. Secondary antibody was applied and cells were washed in a similar manner before imaging.

## Assessment of Endothelial Junctional Integrity

We stained lymphatic vessels for PECAM-1 after three days of simulated obesity or control treatment, as described above. We then imaged the bottom surface at the tips of the vessels with an Achromplan 63×/0.95 NA water immersion objective and counted the number of gaps in PECAM-1 signal along endothelial junctions. Data are from three lymphatics per condition, with 800–1200 µm of junction length analyzed per vessel.

## Quantitative Real-Time PCR

Total RNA was isolated from adipose cells, with or without obesity treatment, using GeneJET RNA purification kit (Thermo Fisher) according to the manufacturer's instructions. cDNA was generated from 0.5 µg of mRNA using LUNA RT Supermix reverse transcript kit (NEB) with a T100 Thermal Cycler (Bio-Rad), according to the manufacturer's instructions. qPCR was performed using LUNA Universal qPCR Master Mix (NEB) with a CFX Opus Real-Time PCR system (Bio-Rad). Relative mRNA levels were calculated using the  $\Delta\Delta\text{CT}$  method using 18S to normalize samples. Primers are listed in Supplementary Table 1.

## Measurement of Collagen Elastic Modulus

To measure the elastic moduli of each collagen gel formulation, we prepared cylindrical discs of gel with a height of ~1 mm and diameter of ~10 mm. Gels were submerged in a solution of 1% BSA in PBS, and stainless steel balls (1.2 mm diameter; Precision Balls) or aluminum balls (1.0 mm diameter; Precision Balls) were carefully placed on top of the gels. The elastic modulus was calculated from the deformation distance of the ball into the gel after 30 min, as described previously [33].

## Statistics

Statistical tests were conducted using Graphpad Prism ver. 5. Solute drainage rates were reported as geometric means with 95% CI and compared using a Mann-Whitney *U* test. Solute retention fractions in the lymphatic vessels were plotted with medians and compared using a Mann-Whitney *U* test. Elastic moduli were reported as mean  $\pm$  SD and compared using one-way ANOVA followed by Dunnett's post-test. Relative mRNA levels and all other continuous data were reported as mean  $\pm$  SD and compared using Welch's or Student's *t* test, respectively. A *p* value of less than 0.05 was considered statistically significant.

## Results

To study how obesity affects lymphatic solute drainage, we adapted a previously developed human lymphatic vessel [23, 24] that was engineered in a micropatterned, cavity-containing type I collagen gel (Fig. 1). We simulated obesity in these vessels by exposing them to a combination of three microenvironmental conditions that are characteristic of obesity: inflammation, hypoxia, and elevated levels of FFAs. We also modified this model to mimic physical or cellular features of the obese adipose tissue microenvironment by crosslinking the collagen gel (i.e., to model a stiffer,

fibrotic tissue) or by embedding adipocytes into the gel. We used 10 ng/mL TNF- $\alpha$  to simulate inflammation, 50  $\mu$ M CoCl<sub>2</sub> to induce a hypoxic response [28], and 0.4 mM oleic acid (with 1% BSA as a carrier) to model hyperlipidemia. For simplicity, “simulated obesity” refers to the addition of TNF- $\alpha$ , CoCl<sub>2</sub>, and oleate to the sample medium, and “obesity-treated lymphatics” or “obesity-treated adipocytes” refers to lymphatics or adipocytes treated with this cocktail, respectively.

### Simulated Obesity Impairs Lymphatic Solute Drainage Independent of Matrix Stiffness

To test whether simulated obesity directly impairs lymphatic solute drainage, we first formed blind-ended lymphatics in uncrosslinked adipocyte-free gels (Fig. 2A and Fig. S1A) and exposed them to TNF- $\alpha$ , CoCl<sub>2</sub>, and oleate. We tested the solute drainage function of the lymphatics after three days of treatment, by adding fluorescent solute to the tip well of the sample and allowing it to drain into the lymphatic under pressure-driven flow for 90 min (Fig. 2B). Drainage rates were calculated from the rate of fluorescence accumulation in the base well, as previously detailed [23, 24]. Solute retention fractions were determined from whole-vessel images taken immediately after the 90-min drainage assay.

We found that simulated obesity impaired solute drainage and caused vessels to become leakier compared to control (Fig. 2C). Simulated obesity reduced solute drainage rate ( $1.8_{-1.1}^{+3.1} \times 10^{-4}$ /min for obesity-treated lymphatics,  $6.9_{-3.7}^{+7.9} \times 10^{-4}$ /min for control lymphatics,  $p = 0.0041$ ; Fig. 2D) and caused less solute to be retained in the lymphatics ( $p = 0.0005$ ; Fig. 2E, F). PECAM-1 staining revealed that control lymphatics exhibited straight, continuous junctions, whereas obesity-treated lymphatics exhibited jagged, discontinuous junctions (Fig. 2G). Obesity-treated lymphatics had more gaps in endothelial junctions ( $24.9 \pm 5.9$  gaps/mm) than control lymphatics did ( $8.4 \pm 3.5$  gaps/mm,  $p = 0.015$ ).

Given that fibrosis often develops in obese adipose tissue, we also tested whether simulated obesity disrupts solute drainage in a stiffer tissue environment (Fig. 3A and Fig. S1B). Here, we crosslinked the collagen gel with genipin before seeding the cavity with LECs. The genipin-crosslinked gels had an elastic modulus of  $1003 \pm 143$  Pa compared to  $108 \pm 21$  Pa for uncrosslinked, acellular gels ( $p < 0.001$ ; Fig. S2).

In crosslinked adipocyte-free gels, simulated obesity again impaired lymphatic solute drainage and caused vessels to become leakier compared to control (Fig. 3B). Simulated obesity reduced solute drainage rate ( $3.9_{-1.3}^{+2.0} \times 10^{-4}$ /min for obesity-treated lymphatics,  $9.6_{-2.0}^{+2.4} \times 10^{-4}$ /min for control lymphatics,  $p = 0.0039$ ; Fig. 3C) and caused less solute to be retained in the lymphatics ( $p = 0.0002$ ; Fig. 3D, E).

Obesity-treated lymphatics had disrupted junctions compared to control lymphatics (Fig. 3F). Obesity-treated lymphatics had more gaps in endothelial junctions ( $36.7 \pm 9.9$  gaps/mm) than control lymphatics did ( $15.2 \pm 3.8$  gaps/mm,  $p = 0.025$ ).

### Conditioned Medium from Obesity-Treated Adipose Cells Does Not Affect Lymphatic Solute Drainage

We expected that obesity-associated conditions could also affect lymphatic drainage function indirectly through changes to surrounding adipocytes. Thus, we first tested whether simulated obesity resulted in changes to adipose cells. We simulated obesity in 2D cultures of differentiated ASCs for three days and compared the gene expression of the obesity-treated adipose cells to that of adipose cells in control conditions. We compared the expression levels of various adipogenic and inflammation-associated genes to validate that the obesity-treated adipose cells were representative of adipocytes in obese tissues *in vivo*. Simulated obesity caused downregulation of the adipogenic genes *PPARG* ( $p = 0.0098$ ), *FABP4* ( $p = 0.0047$ ), and *ADIPOQ* ( $p = 0.0061$ ), but not *PLIN1* ( $p = 0.17$ ), in the adipose cells (Fig. 4). Moreover, simulated obesity caused upregulation of *IL6* ( $p = 0.0065$ ) in the adipose cells. Downregulated expression of adipogenic genes is observed in obesity and could suggest an altered secretome from the obesity-treated cells. Adiponectin, the gene product of *ADIPOQ*, is a secreted adipokine; reduction of adiponectin levels is associated with lymphatic dysfunction [34]. Upregulation of inflammatory cytokines could affect the permeability of lymphatic vessels in a paracrine manner [17, 18].

Given that the obesity-treated adipose cells showed changes in gene expression compared to control, we

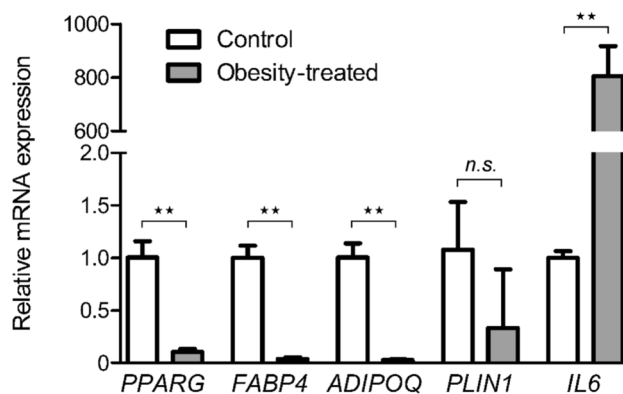


**Fig. 4** Simulated obesity changes adipose cell gene expression. Expression levels of *PPARG*, *FABP4*, *ADIPOQ*, *PLIN1*, and *IL6* in obesity-treated adipose cells are calculated relative to those of untreated (control) adipose cells. Data are from three independent experiments. \*\*,  $p < 0.01$ ; n.s., not significant

wondered if changes in their secreted factors would be sufficient to alter drainage function of engineered lymphatics. To test this idea, we collected CM from obesity-treated or control adipose cells after three days of obesity or mock treatment, respectively. We then formed lymphatic vessels

in crosslinked gels and treated the lymphatics with CM for three days starting on day 5 (Fig. 5A and Fig. S1C). Thus, the lymphatics were exposed to the obesity condition only through obesity-induced alterations in adipose cell-conditioned medium.

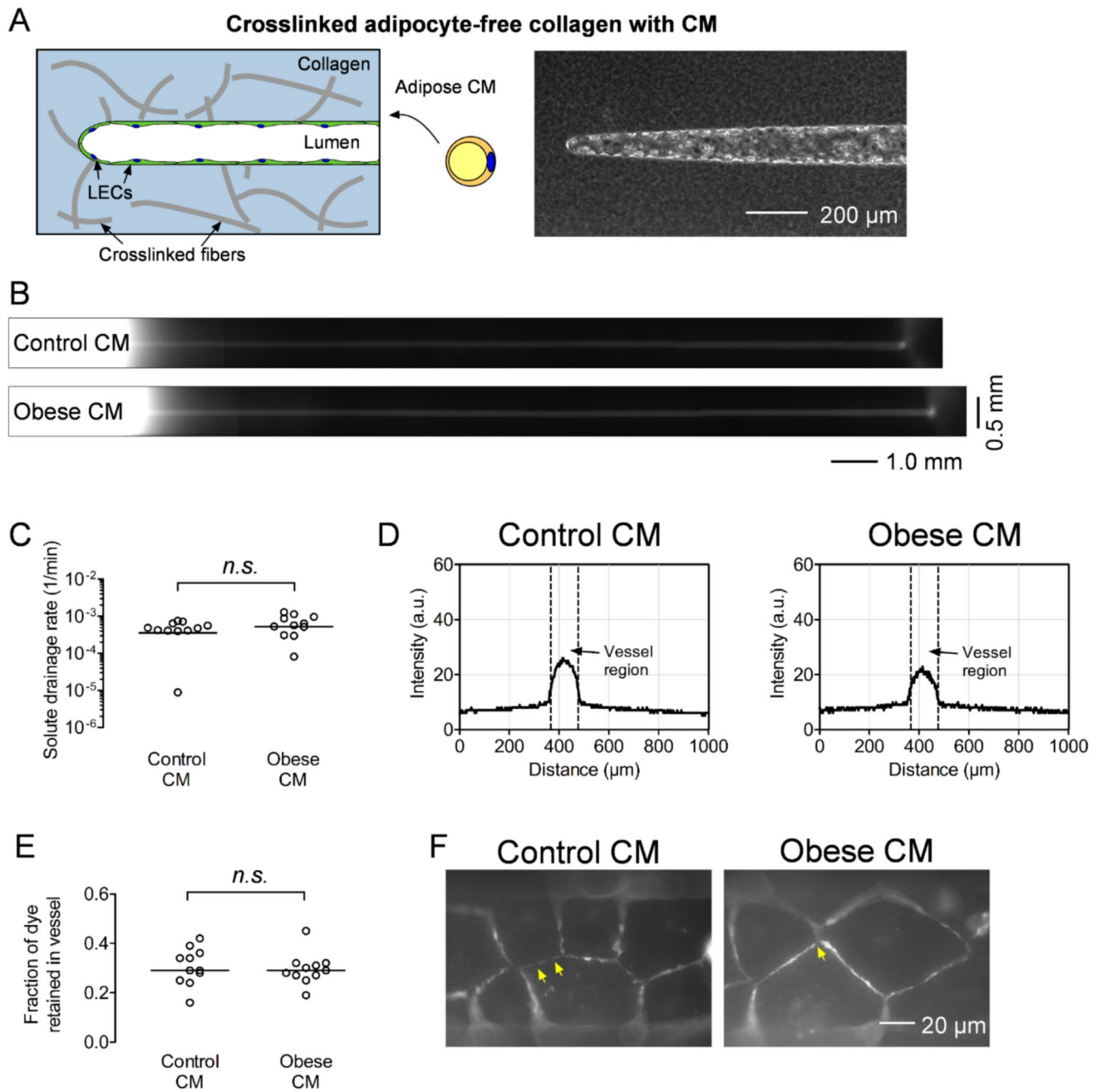


**Fig. 5** CM from obesity-treated adipose cells does not affect lymphatic solute drainage compared to CM from control adipose cells. **A** Schematic (*left*) and phase-contrast image (*right*) of a lymphatic vessel in a crosslinked adipocyte-free collagen gel on day 5. **B** Whole-vessel fluorescence images taken 90 min after introduction of solute. Flow is from left to right. **C** Solute drainage rates. **D** Representative traces of the transverse fluorescence intensity profile, taken 1 cm

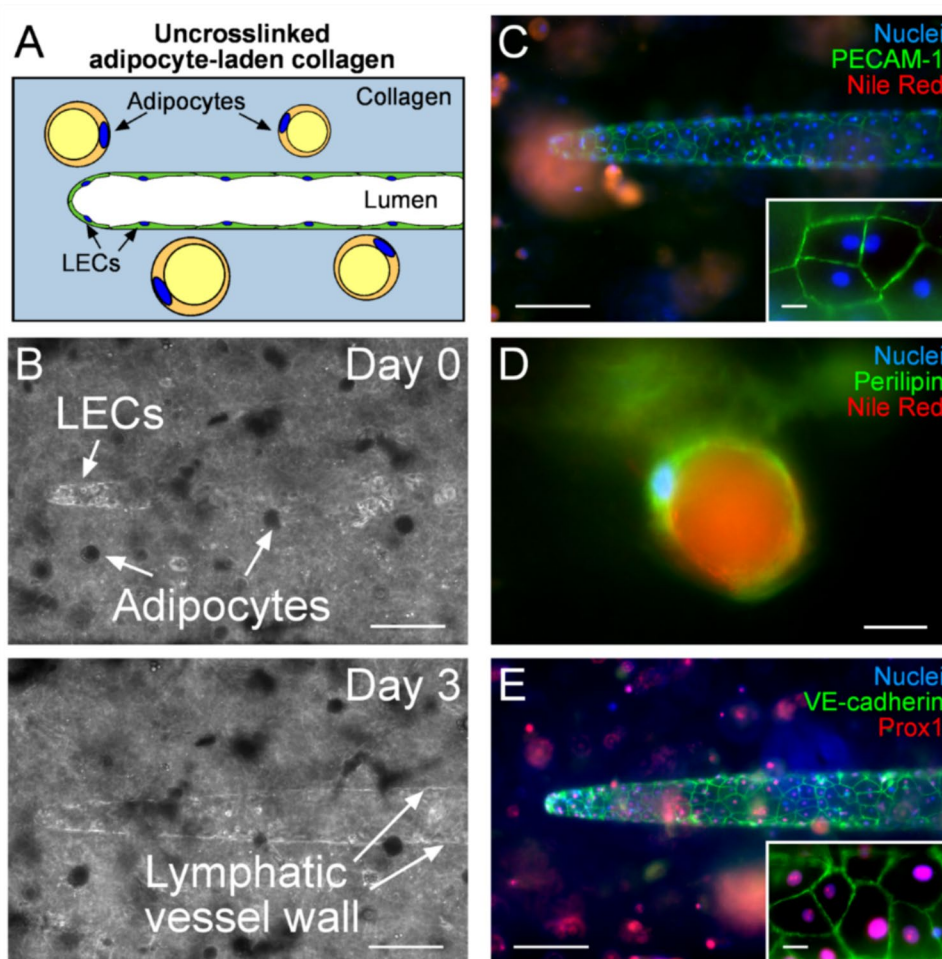
from the open end of the vessel. **E** Solute retention fractions. Data in (**C**) and (**E**) are from six independent experiments. **F** Fluorescence images of lymphatic vessels stained for PECAM-1 on day 8 after three days of treatment with control or obesity-treated CM. Images were taken at the bottom surface of the vessel near the vessel tip. Arrows indicate gaps in junctions. *n.s.*, not significant

We found that CM from obesity-treated adipose cells did not impair solute drainage and did not cause vessels to become leakier compared to CM from control adipose cells (Fig. 5B). CM from obesity-treated adipose cells did not affect solute drainage rate ( $5.3^{+3.7}_{-2.2} \times 10^{-4}$  / min for obesity-treated CM,  $3.6^{+4.7}_{-2.0} \times 10^{-4}$  / min for control CM,  $p=0.29$ ; Fig. 5C) or the amount of solute retained in the lymphatics compared to CM from control adipose cells ( $p=0.65$ ; Fig. 5D, E). CM from obesity-treated adipose cells did not disrupt lymphatic junctions (Fig. 5F). Endothelial junctions of lymphatics that were exposed to obesity-treated CM had  $14.7 \pm 2.0$  gaps/mm, compared to  $13.0 \pm 2.2$  gaps/mm for those of lymphatics that were exposed to control CM ( $p=0.40$ ). These results suggest that any changes to secreted soluble factors in obesity-treated adipose cells compared to control are insufficient to impair lymphatic drainage function.

## Engineering of an Adipose/Lymphatic Co-Culture Model

Even though CM from obesity-treated adipose cells did not affect lymphatic drainage function, it is possible that the presence of obesity-treated adipocytes near the lymphatics could alter function in some other way (i.e., through bidirectional crosstalk with LECs or through physical effects). To study how simulated obesity affects lymphatics in the presence of adipocytes, we first developed a co-culture model that consists of a lymphatic vessel in an adipocyte-laden collagen gel (Fig. 6A). Confluent vessels formed within three days after seeding LECs in cavities in adipocyte-laden gels (Fig. 6B). On average,  $80.0 \pm 1.7\%$  of the adipocytes remained viable on day 3. As we have observed in past work [33], some adipocytes lost lipid and/or dedifferentiated over time. Nile Red stains revealed the fraction of adipocytes that retained lipid (Fig. 6C):  $64.9 \pm 3.9\%$  of the adipocytes remained differentiated (i.e., rounded morphology and positive Nile Red signal) on day 3, compared to  $15.4 \pm 1.8\%$  that had fully dedifferentiated (i.e., elongated morphology and negative Nile Red signal). The remaining  $19.7 \pm 3.4\%$

**Fig. 6** Characterization of adipose/lymphatic co-culture model. **A** Schematic of a lymphatic vessel in an uncrosslinked adipocyte-laden collagen gel. **B** Phase-contrast images on day 0 (*top*) and day 3 (*bottom*). Scale bars refer to 200  $\mu$ m. **C–E** Immunofluorescence images on day 3. **C** PECAM-1/Nile Red stain. Scale bar refers to 200  $\mu$ m. *Inset*, magnified view of the vessel; scale bar refers to 20  $\mu$ m. **D** An embedded adipocyte, stained for Nile Red and perilipin (*green*). Scale bar refers to 20  $\mu$ m. **E** VE-cadherin/Prox1 stain. Scale bar refers to 200  $\mu$ m. *Inset*, magnified view of the vessel; scale bar refers to 20  $\mu$ m. Images are taken at the bottom of the vessel near the vessel tip



of adipocytes had partially dedifferentiated (i.e., elongated morphology or negative Nile Red signal, but not both). As expected, the surface of the lipid droplets stained positively for perilipin (Fig. 6D).

PECAM-1 stains confirmed that the lymphatic endothelium in the co-culture was confluent by day 3 (Fig. 6C), as in adipocyte-free lymphatics. Lymphatics exhibited

continuous PECAM-1 and VE-cadherin signal at endothelial junctions (Fig. 6C, E). The endothelial cells (and some adipocytes) also stained positively for the LEC transcription factor Prox1 (Fig. 6E). Although Prox1 is often viewed as LEC-specific, adipocytes have been reported to express moderate levels of Prox1 compared to other non-endothelial stromal cells [35]; we confirmed positive

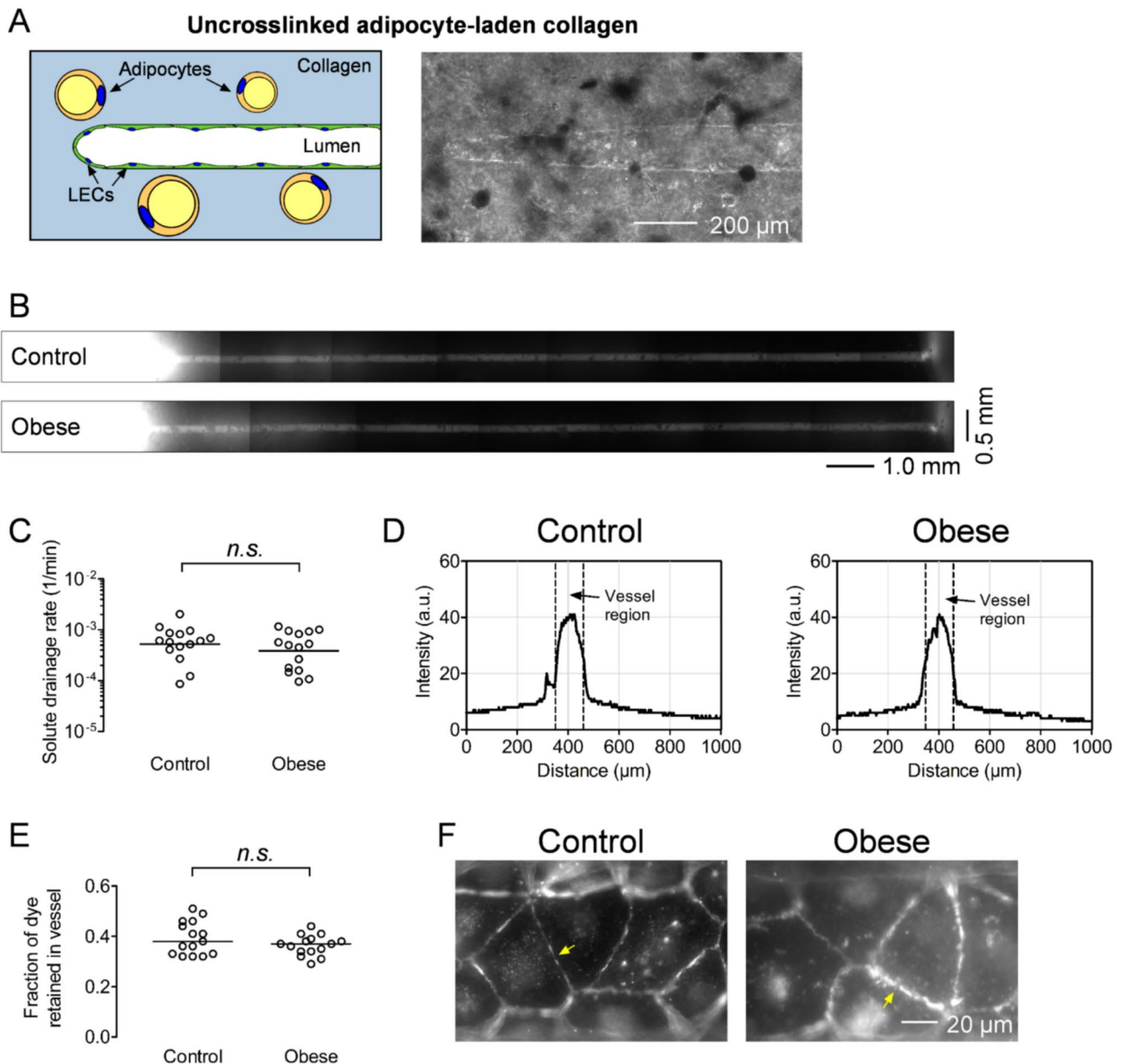


**Fig. 7** Simulated obesity does not impair solute drainage of lymphatics in adipocyte-laden gels. **A** Schematic (*left*) and phase-contrast image (*right*) of a lymphatic vessel in an uncrosslinked adipocyte-laden collagen gel on day 3. **B** Whole-vessel fluorescence images taken 90 min after introduction of solute. Flow is from left to right. **C** Solute drainage rates. **D** Representative traces of the transverse fluorescence intensity profile, taken 1 cm from the open end of the vessel.

**E** Solute retention fractions. Data in (C) and (E) are from ten independent experiments. **F** Fluorescence images of lymphatic vessels stained for PECAM-1 on day 6 after three days of control treatment or simulated obesity. Images were taken at the bottom surface of the vessel near the vessel tip. Arrows indicate gaps in junctions. *n.s.*, not significant

Prox1 expression in adipocytes in 2D culture compared to undifferentiated ASCs (Fig. S3).

### Simulated Obesity Does Not Impair Lymphatic Solute Drainage in Adipocyte-Laden Collagen Gels

To test whether simulated obesity can impair lymphatic solute drainage in the presence of adipocytes, we added TNF- $\alpha$ , CoCl<sub>2</sub>, and oleate to the adipose/lymphatic co-culture model for three days starting on day 3 (Fig. 7A and Fig. S1D). Thus, lymphatics were simultaneously exposed to the conditioned medium of obesity-treated adipocytes in situ and to the obesity treatment directly. We tracked solute drainage in obesity-treated samples and control samples over 90 min (Fig. 7B). Surprisingly, in the presence of adipocytes, simulated obesity did not reduce the solute drainage rate ( $3.9^{+2.4}_{-1.5} \times 10^{-4}$  / min for obesity-treated lymphatics,  $5.3^{+3.0}_{-1.9} \times 10^{-4}$  / min for control lymphatics,  $p=0.43$ ; Fig. 7C) or affect the leakiness ( $p=0.32$ ; Fig. 7D, E) of lymphatics in these co-cultures. Likewise, obesity-treated lymphatics did not exhibit disrupted junctions compared to control lymphatics (Fig. 7F). Endothelial junctions of obesity-treated lymphatics had  $19.3 \pm 6.1$  gaps/mm, compared to  $13.7 \pm 2.1$  gaps/mm for those of control lymphatics ( $p=0.21$ ).

## Discussion

In the current study, we developed and used 3D in vitro models of lymphatic vessels with or without adipocytes to study how obesity affects lymphatic solute drainage. To model an obese microenvironment, we added TNF- $\alpha$ , CoCl<sub>2</sub>, and oleate to simulate inflammation, hypoxia, and elevated FFA levels, respectively. We used a previously developed solute drainage assay, similar to lymphoscintigraphy in vivo, to measure solute drainage rates of the lymphatic vessels [23]. We found that simulated obesity impaired lymphatic solute drainage in a soft or stiff matrix in the absence of adipocytes (Figs. 2 and 3), but did not affect drainage in the presence of adipocytes (Fig. 7). Moreover, CM from obesity-treated adipose cells did not affect lymphatic solute drainage (Fig. 5).

### Design Rationale for the Tissue-Engineered Lymphatic Model

Although other studies have developed microphysiological systems to investigate the interactions of adipose and vessels [36, 37], our model is distinct in that it uses human cells, incorporates a 3D blind-ended lymphatic vessel, and enables the measurement of physiological parameters such as solute drainage rate and leakage. Adipocytes are appropriate cells to include in this model because they are often found in close proximity to lymphatic vessels, are involved

with the development of microenvironmental changes associated with obesity (e.g., hypoxia, chronic inflammation, and hyperlipidemia), and are known to secrete factors (e.g., adipokines) that may alter lymphatic function [38]. The inclusion of adipocytes allowed us to investigate how simulated obesity could alter adipocytes in a co-culture model and whether those changes could further impact lymphatic drainage function.

We used adipocytes that were differentiated from telomericized human ASCs to allow for better reproducibility of the model compared to one that uses primary human ASCs. These immortalized precursor cells have been demonstrated to express similar levels of the adipogenic marker *PPARG* compared to their original primary cells [22]. The ASC-derived adipocytes in our model are smaller ( $47.4 \pm 15.9$   $\mu$ m in diameter) than hypertrophic adipocytes in obese humans (100–150  $\mu$ m in diameter) in vivo but comparable in size to primary ASC-derived adipocytes [29]. Adipocyte-laden gels had an elastic modulus of  $106 \pm 17$  Pa, which was comparable to that of uncrosslinked, acellular gels ( $p > 0.05$ ; Fig. S2).

### Comparison of Obesity-Induced Changes in Lymphatic Solute Drainage In Vivo and In Vitro

Consistent with our findings in vitro, several studies have reported impairment of solute drainage in the lymphatics of obese mice and humans. Patients with very high BMI (>55) have abnormal lymphoscintigraphy results, which suggests that morbid obesity is linked to lymphatic dysfunction [3]. In a mouse model of diet-induced obesity, obese mice have poorer solute drainage to the inguinal lymph node [39]. While the reduction in solute drainage can be a direct consequence of reduced contractility (and the resulting lower fluid drainage rates), our model instead allowed us to investigate whether the obese tissue microenvironment can impair solute drainage independently of changes in fluid drainage rates. We found that obesity-treated lymphatics exhibited lower solute drainage rates, which correlated with increased solute leakage and disrupted endothelial junctions. Our data imply that obesity-associated conditions can impair lymphatic solute drainage function directly by damaging lymphatic junctions.

It may seem counterintuitive that leakier lymphatics drain more poorly. After all, a lymphatic can only drain properly if its endothelium is permeable. Generalized leakiness throughout the entire lymphatic network, however, is not conducive to drainage. Rather, segmental differences in permeability—in which the blind end of the lymphatic is leaky, while the remainder of the vessel is not—appear to be crucial for effective solute drainage [23]. Consistent with this idea, some studies have reported that obesity can cause solute leakage from lymphatics in vivo, mainly

in the gut microcirculation [16, 40]. Mesenteric lymphatic vessels, which lie within adipose-rich stroma, are leaky in obese mice and humans, which results in accumulation of lipids in the interstitium and poor drainage of dietary lipids, lipophilic drugs, and antigens to mesenteric lymph nodes.

### Role of Obesity-Associated Conditions in Obesity-Induced Lymphatic Dysfunction

Our results show that obesity-associated conditions act directly on lymphatic vessels to disrupt endothelial junctions, promote leakage, and impair solute drainage (Figs. 2 and 3). This direct effect is independent of matrix stiffness, at least within the range of moduli that was studied here (i.e., 100–1000 Pa). Past studies have shown that TNF- $\alpha$ , hypoxia, and FFAs separately influence lymphatic function by either weakening or strengthening endothelial junctions or by promoting lymphangiogenesis [17, 19–21]. To our knowledge, their combined effect on lymphatic physiology has not been explored previously.

TNF- $\alpha$  is one of the major pro-inflammatory cytokines elevated in adipose tissue during obesity [12]. Macrophages, which accumulate in adipose tissue as obesity progresses, are thought to be the main source of TNF- $\alpha$  in obese tissues [41, 42]. TNF- $\alpha$  alters the morphology of LECs, disrupts endothelial junctions, and decreases endothelial barrier function [17, 19]. The greater number of gaps observed in endothelial junctions in our obesity-treated lymphatics is consistent with the discontinuous junctions in LEC monolayers that are treated with TNF- $\alpha$  [19]. The increased solute leakage from the obesity-treated lymphatics agrees with previous reports of reduced transendothelial electrical resistance and increased permeability of LEC monolayers treated with TNF- $\alpha$  [17, 19].

Hypoxia in obesity is caused by the rapid expansion of adipose tissue relative to vascular growth [9]. Hypoxia promotes lymphangiogenesis via activation of HIF-1 $\alpha$  in LECs [43], and inhibition of HIF-1 $\alpha$  activity slows lymphatic recovery in a mouse tail model of lymphedema [44]. We did not observe any lymphangiogenesis in either control or obesity-treated lymphatics. Tatin et al. found that LECs in a hypoxic chamber had less VE-cadherin at endothelial junctions than LECs under normoxic conditions did [45]. While we did not investigate VE-cadherin localization or expression in obesity-treated lymphatics, the gaps in PECAM-1 signal that we observed in the junctions are consistent with these findings.

Elevated FFA concentration is typical in obesity and can arise from lipid intake and from increased lipolysis in adipose tissue [14]. We chose to use oleate, an unsaturated FFA, because it is the most abundant FFA in human adipose tissue and its levels are elevated in obesity [46, 47]. Oleate increases the permeability of LEC monolayers by causing

gaps in VE-cadherin localization at endothelial junctions [48]. Nevertheless, it is important to recognize that different FFAs—whether singly or in combination—can affect lymphatic function in different ways. Palmitate, a saturated FFA, can promote vascular cell apoptosis and inflammation and can destabilize junctions in human LECs [21, 49]. Stearate, another saturated FFA, slows cell growth and induces an inflammatory response in human aortic endothelial cells, but oleate can inhibit the effect of stearate [50]. In our model, the poor barrier function of the obesity-treated lymphatics suggests that the addition of oleate either contributed to disruption of endothelial junctions or, at the very least, was insufficient to protect against junctional damage from other causes.

Tissue fibrosis often results from chronic inflammation and the resulting overactive repair mechanisms and excessive deposition of matrix proteins [51]. Matrix stiffening from fibrosis has been shown to affect lymphatic function, including the worsening of lymphedema [52]. Increasing matrix stiffness causes ECs to reorganize the actin cytoskeleton, which affects VE-cadherin localization and junction stability [53]. Our results show that simulated obesity impairs lymphatic drainage function, whether in a matrix with an elastic modulus of  $\sim 100$  Pa or  $\sim 1000$  Pa. This finding implies that the effect of the obesity treatment dominates any changes in drainage function that may result from differences in matrix stiffness, at least in the range of stiffnesses considered here.

### Role of Adipose Cells in Obesity-Induced Lymphatic Dysfunction

We found that adipose cells that were exposed to simulated obesity expressed lower levels of the adipogenic genes *PPARG*, *FABP4*, and *ADIPOQ* and a higher level of the inflammatory gene *IL6* (Fig. 4). The gene expression differences of our obesity-treated adipose cells match closely to those reported for adipocytes that are exposed separately to hypoxia or TNF- $\alpha$  and are mostly consistent with that of adipocytes in obese adipose tissue. For instance, adiponectin levels in obese patients are normally decreased [54]. Hypoxia inhibits *PPARG*, *FABP4*, and *ADIPOQ* expression in vitro [55]. *ADIPOQ* and *PPARG* expression are also inhibited by inflammatory factors, particularly TNF- $\alpha$  [56]. Obesity causes an increase in the production of inflammatory cytokines, such as IL-6, in adipose tissue [57].

Given the lower *ADIPOQ* expression and higher *IL6* expression of our obesity-treated adipose cells, we expected that the obesity-treated adipose cells would contribute to lymphatic dysfunction from CM alone or in our co-culture model. Low adiponectin levels are associated with lymphatic dysfunction in vivo [34], while IL-6 is known to increase the permeability of lymphatic

endothelium in vitro [17, 18]. Surprisingly, we found that the presence of adipocytes *protected* the lymphatics from the detrimental effects of obesity-associated conditions (Fig. 7). Moreover, CM from obesity-treated adipose cells did not impair lymphatic drainage function (Fig. 5). Collectively, these results suggest that the mixture of soluble factors from obese adipose cells does not impair lymphatic solute drainage overall.

One possible explanation for the unimpaired lymphatic drainage function after simulated obesity in our co-culture model is that bidirectional interactions between adipocytes and LECs could result in the production of junction-stabilizing factors, such as VEGF-A [58], which could counter the effects of the obesity-associated conditions on LECs. Some adipokines, such as apelin and adrenomedullin, can stabilize lymphatic endothelium and could be responsible for the observed protective role of adipocytes [48, 59].

It is also possible that we did not find a negative effect of the obesity-treated adipocytes on lymphatic drainage because the density of adipocytes in the in vitro model was low. The volume fraction of adipocytes in adipose tissue typically exceeds 90% [60], whereas the volume fraction of adipocytes in our model is below ~2%. In addition, the exposure of adipocytes and LECs to simulated obesity is short (only three days) and may not be reflective of adipose tissue in which obesity develops over years. Although these differences could in principle diminish any adipocyte-dependent effect in our model, we have shown that similar adipocyte densities are sufficient to alter behavior in other 3D microscale tissue models [29, 33]. Moreover, the density of adipocytes used in this study was able to abrogate the effect of obesity treatment on drainage. Regardless of the underlying reason, our data indicate the direct effect of the obese microenvironment on lymphatics is critical for derangements in solute drainage.

## Potential Implications

Our findings imply that obesity-associated conditions can impair lymphatic solute drainage and promote leakage via disruption of lymphatic junctions. This finding suggests that therapies that target the junctional response of lymphatic endothelium to inflammation, hypoxia, or fatty acid levels, rather than targeting the adipocytes per se, could improve solute drainage function in obese patients. Given that the presence of adipocytes eliminated the negative effects of obesity on solute drainage function, it is worth exploring how adipocytes and/or their secreted factors can protect lymphatic endothelial junctions from obesity-induced damage.

## Limitations of the Model

Although our work modeled the obese microenvironment as a combination of inflammation, hypoxia, and hyperlipidemia, we only used one factor to induce each feature (e.g., TNF- $\alpha$  for inflammation). We did not determine if a subset of factors was sufficient for the observed effects on solute drainage, nor do we know whether these factors act synergistically or independently. Moreover, our experiments did not capture other obesity-related perturbations, such as hyperinsulinemia. Hyperinsulinemia can induce insulin resistance and impaired barrier function in LECs; if anything, we would expect the addition of excess insulin to accentuate the negative effect of obesity-associated conditions on lymphatic solute drainage [61]. Obesity is not a homogeneous condition [62, 63], and modeling different types of obesity (e.g., leptin-dependent versus leptin-independent) will require modifications of the model.

In terms of the cellular and physical aspects of the model, one limitation is the absence of immune cells, such as macrophages, in the collagen gel that surrounds the lymphatic vessel. Obesity-associated conditions can induce a positive feedback loop between adipocytes and macrophages that amplifies the inflammatory state [64]; such crosstalk is not present in our model. Another limitation is that our work used only type I collagen to model the adipose matrix, which does not fully capture the complexity of the extracellular matrix in human adipose tissue or obesity-associated changes in matrix composition. Future models can incorporate other matrix components, such as collagen IV or collagen VI (which is upregulated in obesity [65]), to better mimic adipose tissue [66]. Also, our lymphatics are not subjected to oscillatory flow that would create more realistic time-dependent pressure gradients and flow profiles during drainage. These limitations suggest obvious next steps for enhancing the physiological faithfulness of the model.

## Conclusions

In this study, we simulated obesity-associated inflammation, hypoxia, and tissue hyperlipidemia in 3D engineered models of human lymphatics and showed that these combined conditions directly disrupt endothelial junctions, increase solute leakage from lymphatics, and impair lymphatic solute drainage. These findings suggest a potential mechanism by which the obesity-associated microenvironment can impair solute drainage through its effects on endothelial junctions. Surprisingly, the presence of adipocytes prevented the obesity-mediated deterioration in

lymphatic drainage, and CM from obesity-treated adipose cells did not affect lymphatic drainage. These findings reveal a protective role of adipocytes on obesity-associated lymphatic dysfunction that will need to be explored further. Normalizing the dysfunctional obese tissue microenvironment by reducing inflammation, hypoxia, and/or FFA concentrations may prevent junctional damage and improve solute drainage function. Alternatively, strengthening lymphatic junctions may help maintain drainage in an obese environment. These findings also indicate that targeting signaling pathways related to inflammation, hypoxia, and/or lipid transport in the lymphatics may be a better strategy to improve solute drainage in obese patients, compared to targeting similar pathways in adipocytes. More broadly, our study provides an example of how engineered human 3D vascular models can be used to study the interactions of vessels and their environment in the context of obesity or other metabolic disorders.

**Supplementary Information** The online version contains supplementary material available at <https://doi.org/10.1007/s12195-024-00840-z>.

**Acknowledgments** This study was funded by a Dean's Catalyst Award from Boston University. M.D.L. and C.L.F. were supported by award R01 DK132080 from the National Institute of Diabetes and Digestive and Kidney Diseases. A.R.T., N.L., and J.A.B. were funded by the Undergraduate Research Opportunities Program at Boston University. We thank Yoseph W. Dance for helpful discussions and Owen M. Kelly and Yixin Gao for assistance with experiments.

**Funding** This study was funded by National Institute of Diabetes and Digestive and Kidney Diseases, R01DK132080, Matthew D. Layne.

**Data availability** Data will be made available upon request.

## Declarations

**Conflict of interest** Alex J. Seibel, Cheyanne L. Frosti, Abderrahman R. Tlemçani, Nikhil Lahiri, Joely A. Brammer-DePuy, Matthew D. Layne, and Joe Tien declare that they have no conflict of interest.

**Ethical Approval** No human or animal studies were carried out by the authors for this article.

## References

- Kataru, R. P., H. J. Park, J. E. Baik, C. Li, J. Shin, and B. J. Mehrara. Regulation of lymphatic function in obesity. *Front. Physiol.* 11:459, 2020.
- Arngrim, N., L. Simonsen, J. J. Holst, and J. Bulow. Reduced adipose tissue lymphatic drainage of macromolecules in obese subjects: a possible link between obesity and local tissue inflammation? *Int. J. Obes.* 37:748–751, 2013.
- Greene, A. K., F. D. Grant, and S. A. Slavin. Lower-extremity lymphedema and elevated body-mass index. *N. Engl. J. Med.* 366:2136–2137, 2012.
- Mehrara, B. J., and A. K. Greene. Lymphedema and obesity: is there a link? *Plast. Reconstr. Surg.* 134:154e–160e, 2014.
- Greene, A. K., F. D. Grant, and R. A. Maclellan. Obesity-induced lymphedema nonreversible following massive weight loss. *Plast. Reconstr. Surg. Glob. Open* 3:e426, 2015.
- Marcelin, G., E. L. Gautier, and K. Clément. Adipose tissue fibrosis in obesity: etiology and challenges. *Annu. Rev. Physiol.* 84:135–155, 2022.
- Crewe, C., Y. A. An, and P. E. Scherer. The ominous triad of adipose tissue dysfunction: inflammation, fibrosis, and impaired angiogenesis. *J. Clin. Invest.* 127:74–82, 2017.
- Trayhurn, P. Hypoxia and adipose tissue function and dysfunction in obesity. *Physiol. Rev.* 93:1–21, 2013.
- Pasarica, M., O. R. Sereda, L. M. Redman, D. C. Albarado, D. T. Hymel, L. E. Roan, J. C. Rood, D. H. Burk, and S. R. Smith. Reduced adipose tissue oxygenation in human obesity. *Diabetes* 58:718–725, 2009.
- Cancello, R., and K. Clément. Is obesity an inflammatory illness? role of low-grade inflammation and macrophage infiltration in human white adipose tissue. *Br. J. Obstet. Gynaecol.* 113:1141–1147, 2006.
- Divoux, A., J. Tordjman, D. Lacasa, N. Veyrie, D. Hugol, A. Aïssat, A. Basdevant, M. Guerre-Millo, C. Poitou, J.-D. Zucker, P. Bedossa, and K. Clément. Fibrosis in human adipose tissue: composition, distribution, and link with lipid metabolism and fat mass loss. *Diabetes* 59:2817–2825, 2010.
- Hotamisligil, G. S., P. Arner, J. F. Caro, R. L. Atkinson, and B. M. Spiegelman. Increased adipose tissue expression of tumor necrosis factor- $\alpha$  in human obesity and insulin resistance. *J. Clin. Invest.* 95:2409–2415, 1995.
- Wueest, S., R. A. Rapold, J. M. Rytka, E. J. Schoenle, and D. Konrad. Basal lipolysis, not the degree of insulin resistance, differentiates large from small isolated adipocytes in high-fat fed mice. *Diabetologia* 52:541–546, 2009.
- Boden, G. Obesity and free fatty acids (FFA). *Endocrinol. Metab. Clin.* 37:635–646, 2008.
- Torrisi, J. S., G. E. Hespe, D. A. Cuzzone, I. L. Savetsky, M. D. Nitti, J. C. Gardenier, G. D. G. Nores, D. Jowhar, R. P. Kataru, and B. J. Mehrara. Inhibition of inflammation and iNOS improves lymphatic function in obesity. *Sci. Rep.* 6:19817, 2016.
- Cao, E., M. J. Watt, C. J. Nowell, T. Quach, J. S. Simpson, V. De Melo Ferreira, S. Agarwal, H. Chu, A. Srivastava, D. Anderson, G. Gracia, A. Lam, G. Segal, J. Hong, L. Hu, K. L. Phang, A. B. J. Escott, J. A. Windsor, A. R. J. Phillips, D. J. Creek, N. L. Harvey, C. J. H. Porter, and N. L. Trevaskis. Mesenteric lymphatic dysfunction promotes insulin resistance and represents a potential treatment target in obesity. *Nat. Metab.* 3:1175–1188, 2021.
- Cromer, W. E., S. D. Zawieja, B. Tharakan, E. W. Childs, M. K. Newell, and D. C. Zawieja. The effects of inflammatory cytokines on lymphatic endothelial barrier function. *Angiogenesis* 17:395–406, 2014.
- Gong, M. M., K. M. Lugo-Cintron, B. R. White, S. C. Kerr, P. M. Harari, and D. J. Beebe. Human organotypic lymphatic vessel model elucidates microenvironment-dependent signaling and barrier function. *Biomaterials* 214:119225, 2019.
- Kakei, Y., M. Akashi, T. Shigeta, T. Hasegawa, and T. Komori. Alteration of cell–cell junctions in cultured human lymphatic endothelial cells with inflammatory cytokine stimulation. *Lymphat. Res. Biol.* 12:136–143, 2014.
- Morfoisse, F., E. Renaud, F. Hantelys, A.-C. Prats, and B. Garmy-Susini. Role of hypoxia and vascular endothelial growth factors in lymphangiogenesis. *Mol. Cell. Oncol.* 2:e1024821, 2015.
- Tokarz, V. L., R. V. S. Pereira, J. R. Jaldin-Fincati, S. Mylvaganam, and A. Klip. Junctional integrity and directional mobility of lymphatic endothelial cell monolayers are disrupted by saturated fatty acids. *Mol. Biol. Cell* 34:ar28, 2023.
- Xue, R., M. D. Lynes, J. M. Dreyfuss, F. Shamsi, T. J. Schulz, H. Zhang, T. L. Huang, K. L. Townsend, Y. Li, H. Takahashi, L. S.

- Weiner, A. P. White, M. S. Lynes, L. L. Rubin, L. J. Goodyear, A. M. Cypess, and Y.-H. Tseng. Clonal analyses and gene profiling identify genetic biomarkers of the thermogenic potential of human brown and white preadipocytes. *Nat. Med.* 21:760–768, 2015.
23. Thompson, R. L., E. A. Margolis, T. J. Ryan, B. J. Coisman, G. M. Price, K. H. K. Wong, and J. Tien. Design principles for lymphatic drainage of fluid and solutes from collagen scaffolds. *J. Biomed. Mater. Res. A* 106:106–114, 2018.
  24. Tien, J., and U. Ghani. Methods for forming human lymphatic microvessels in vitro and assessing their drainage function. In: *Biomedical Engineering Technologies*, edited by A. Rasooly, H. Baker, and M. R. Ossandon. Springer, 2022, pp. 651–668.
  25. Leung, A. D., K. H. K. Wong, and J. Tien. Plasma expanders stabilize human microvessels in microfluidic scaffolds. *J. Biomed. Mater. Res. A* 100A:1815–1822, 2012.
  26. Duncan, R. E., M. Ahmadian, K. Jaworski, E. Sarkadi-Nagy, and H. S. Sul. Regulation of lipolysis in adipocytes. *Annu. Rev. Nutr.* 27:79–101, 2007.
  27. Wong, K. H. K., J. G. Truslow, and J. Tien. The role of cyclic AMP in normalizing the function of engineered human blood microvessels in microfluidic collagen gels. *Biomaterials* 31:4706–4714, 2010.
  28. Yuan, Y., G. Hilliard, T. Ferguson, and D. E. Millhorn. Cobalt inhibits the interaction between hypoxia-inducible factor- $\alpha$  and von Hippel-Lindau protein by direct binding to hypoxia-inducible factor- $\alpha$ . *J. Biol. Chem.* 278:15911–15916, 2003.
  29. Dance, Y. W., M. C. Obenreder, A. J. Seibel, T. Meshulam, J. W. Ogony, N. Lahiri, L. Pacheco-Spann, D. C. Radisky, M. D. Layne, S. R. Farmer, C. M. Nelson, and J. Tien. Adipose cells induce escape from an engineered human breast microtumor independently of their obesity status. *Cell. Mol. Bioeng.* 16:23–39, 2023.
  30. Modi, S., A. W. B. Stanton, W. E. Svensson, A. M. Peters, P. S. Mortimer, and J. R. Levick. Human lymphatic pumping measured in healthy and lymphoedematous arms by lymphatic congestion lymphoscintigraphy. *J. Physiol.* 583:271–285, 2007.
  31. Piotrowski-Daspiet, A. S., A. K. Simi, M.-F. Pang, J. Tien, and C. M. Nelson. A 3D culture model to study how fluid pressure and flow affect the behavior of aggregates of epithelial cells. In: *Mammary Gland Development*, edited by F. Martin, T. Stein, and J. Howlin. New York: Springer, 2017, pp. 245–257.
  32. Seibel, A. J., O. M. Kelly, Y. W. Dance, C. M. Nelson, and J. Tien. Role of lymphatic endothelium in vascular escape of engineered human breast microtumors. *Cell. Mol. Bioeng.* 15:553–569, 2022.
  33. Dance, Y. W., T. Meshulam, A. J. Seibel, M. C. Obenreder, M. D. Layne, C. M. Nelson, and J. Tien. Adipose stroma accelerates the invasion and escape of human breast cancer cells from an engineered microtumor. *Cell. Mol. Bioeng.* 15:15–29, 2022.
  34. Shimizu, Y., R. Shibata, M. Ishii, K. Ohashi, T. Kambara, Y. Uemura, D. Yuasa, Y. Kataoka, S. Kihara, T. Murohara, and N. Ouchi. Adiponectin-mediated modulation of lymphatic vessel formation and lymphedema. *J. Am. Heart Assoc.* 2:e000438, 2013.
  35. Karlsson, M., C. Zhang, L. Méar, W. Zhong, A. Digre, B. Katona, E. Sjöstedt, L. Butler, J. Odeberg, P. Dusart, F. Edfors, P. Oksvold, K. von Feilitzen, M. Zwahlen, M. Arif, O. Altay, X. Li, M. Ozcan, A. Mardonoglu, L. Fagerberg, J. Mulder, Y. Luo, F. Ponten, M. Uhlén, and C. Lindskog. A single-cell type transcriptomics map of human tissues. *Sci. Adv.* 7:eabh2169, 2021.
  36. Li, X., J. Xia, C. T. Nicolescu, M. W. Massidda, T. J. Ryan, and J. Tien. Engineering of microscale vascularized fat that responds to perfusion with lipoactive hormones. *Biofabrication* 11:014101, 2018.
  37. Paek, J., S. E. Park, Q. Lu, K.-T. Park, M. Cho, J. M. Oh, K. W. Kwon, Y.-S. Yi, J. W. Song, H. I. Edelstein, J. Ishibashi, W. Yang, J. W. Myerson, R. Y. Kiseleva, P. Aprelev, E. D. Hood, D. Stambolian, P. Seale, V. R. Muzykantov, and D. Huh. Microphysiological engineering of self-assembled and perfusable microvascular beds for the production of vascularized three-dimensional human microtissues. *ACS Nano* 13:7627–7643, 2019.
  38. Ouchi, N., J. L. Parker, J. J. Lugus, and K. Walsh. Adipokines in inflammation and metabolic disease. *Nat. Rev. Immunol.* 11:85–97, 2011.
  39. Nitti, M. D., G. E. Hespe, R. P. Kataru, G. D. García Nores, I. L. Savetsky, J. S. Torrisi, J. C. Gardenier, A. J. Dannenberg, and B. J. Mehrara. Obesity-induced lymphatic dysfunction is reversible with weight loss. *J. Physiol.* 594:7073–7087, 2016.
  40. Mikrani, R., I. K. Styles, T. A. Hoang, M. Abdallah, D. Senyschyn, C. J. H. Porter, E. Cao, and N. L. Trevaskis. Obesity-associated mesenteric lymph leakage impairs the trafficking of lipids, lipophilic drugs and antigens from the intestine to mesenteric lymph nodes. *Eur. J. Pharm. Biopharm.* 180:319–331, 2022.
  41. Xu, H., G. T. Barnes, Q. Yang, G. Tan, D. Yang, C. J. Chou, J. Sole, A. Nichols, J. S. Ross, L. A. Tartaglia, and H. Chen. Chronic inflammation in fat plays a crucial role in the development of obesity-related insulin resistance. *J. Clin. Invest.* 112:1821–1830, 2003.
  42. Weisberg, S. P., D. McCann, M. Desai, M. Rosenbaum, R. L. Leibel, and A. W. Ferrante. Obesity is associated with macrophage accumulation in adipose tissue. *J. Clin. Invest.* 112:1796–1808, 2003.
  43. Jiang, X., W. Tian, D. Kim, A. S. McQuiston, R. Vinh, S. G. Rockson, G. L. Semenza, and M. R. Nicolls. Hypoxia and hypoxia-inducible factors in lymphedema. *Front. Pharmacol.* 13:851057, 2022.
  44. Zampell, J. C., A. Yan, T. Avraham, S. Daluvoy, E. S. Weitman, and B. J. Mehrara. HIF-1 $\alpha$  coordinates lymphangiogenesis during wound healing and in response to inflammation. *FASEB J.* 26:1027–1039, 2012.
  45. Tatin, F., E. Renaud-Gabardos, A.-C. Godet, F. Hantelys, F. Pujol, F. Morfoisse, D. Calise, F. Viars, P. Valet, B. Masri, A.-C. Prats, and B. Garmy-Susini. Apelin modulates pathological remodeling of lymphatic endothelium after myocardial infarction. *JCI Insight* 2:e93887, 2017.
  46. Hodson, L., C. M. Skeaff, and B. A. Fielding. Fatty acid composition of adipose tissue and blood in humans and its use as a biomarker of dietary intake. *Prog. Lipid Res.* 47:348–380, 2008.
  47. Newgard, C. B., J. An, J. R. Bain, M. J. Muehlbauer, R. D. Stevens, L. F. Lien, A. M. Haqq, S. H. Shah, M. Arlotto, C. A. Slentz, J. Rochon, D. Gallup, O. Ilkayeva, B. R. Wenner, W. E. Yancy, H. Eissenon, G. Musante, R. Surwit, D. S. Millington, M. D. Butler, and L. P. Svetkey. A branched-chain amino acid-related metabolic signature that differentiates obese and lean humans and contributes to insulin resistance. *Cell Metab.* 9:311–326, 2009.
  48. Sawane, M., K. Kajiya, H. Kidoya, M. Takagi, F. Muramatsu, and N. Takakura. Apelin inhibits diet-induced obesity by enhancing lymphatic and blood vessel integrity. *Diabetes* 62:1970–1980, 2013.
  49. Harvey, K. A., C. L. Walker, T. M. Pavlina, Z. Xu, G. P. Zaloga, and R. A. Siddiqui. Long-chain saturated fatty acids induce pro-inflammatory responses and impact endothelial cell growth. *Clin. Nutr.* 29:492–500, 2010.
  50. Harvey, K. A., C. L. Walker, Z. Xu, P. Whitley, T. M. Pavlina, M. Hise, G. P. Zaloga, and R. A. Siddiqui. Oleic acid inhibits stearic acid-induced inhibition of cell growth and pro-inflammatory responses in human aortic endothelial cells. *J. Lipid Res.* 51:3470–3480, 2010.
  51. Wynn, T. Cellular and molecular mechanisms of fibrosis. *J. Pathol.* 214:199–210, 2008.
  52. Kataru, R. P., I. Wiser, J. E. Baik, H. J. Park, S. Rehal, J. Shin, and B. J. Mehrara. Fibrosis and secondary lymphedema: chicken or egg? *Transl. Res.* 209:68–76, 2019.
  53. Bordeleau, F., B. N. Mason, E. M. Lollis, M. Mazzola, M. R. Zanotelli, S. Somasegar, J. P. Califano, C. Montague, D. J.

- LaValley, J. Huynh, N. Mencia-Trinchant, Y. L. Negrón Abril, D. C. Hassane, L. J. Bonassar, J. T. Butcher, R. S. Weiss, and C. A. Reinhart-King. Matrix stiffening promotes a tumor vasculature phenotype. *Proc. Natl. Acad. Sci. USA* 114:492–497, 2017.
54. Nigro, E., O. Scudiero, M. L. Monaco, A. Palmieri, G. Mazzarella, C. Costagliola, A. Bianco, and A. Daniele. New insight into adiponectin role in obesity and obesity-related diseases. *Biomed. Res. Int.* 2014:658913, 2014.
55. Anvari, G., and E. Bellas. Hypoxia induces stress fiber formation in adipocytes in the early stage of obesity. *Sci. Rep.* 11:21473, 2021.
56. Cawthorn, W. P., and J. K. Sethi. TNF- $\alpha$  and adipocyte biology. *FEBS Lett.* 582:117–131, 2008.
57. Trayhurn, P., and I. S. Wood. Adipokines: inflammation and the pleiotropic role of white adipose tissue. *Br. J. Nutr.* 92:347–355, 2004.
58. Zhang, F., G. Zarkada, J. Han, J. Li, A. Dubrac, R. Ola, G. Genet, K. Boyé, P. Michon, S. E. Künzel, J. P. Camporez, A. K. Singh, G.-H. Fong, M. Simons, P. Tso, C. Fernández-Hernando, G. I. Shulman, W. C. Sessa, and A. Eichmann. Lacteal junction zippering protects against diet-induced obesity. *Science* 361:599–603, 2018.
59. Xu, W., E. S. Wittchen, S. L. Hoopes, L. Stefanini, K. BurrIDGE, and K. M. Caron. Small GTPase Rap1A/B is required for lymphatic development and adrenomedullin-induced stabilization of lymphatic endothelial junctions. *Arterioscler. Thromb. Vasc. Biol.* 38:2410–2422, 2018.
60. Corvera, S. Cellular heterogeneity in adipose tissues. *Annu. Rev. Physiol.* 83:257–278, 2021.
61. Lee, Y., S. Chakraborty, C. J. Meininger, and D. M. Muthuchamy. Insulin resistance disrupts cell integrity, mitochondrial function and inflammatory signaling in lymphatic endothelium. *Microcirculation* 25:e12492, 2018.
62. Blüher, M. Obesity: global epidemiology and pathogenesis. *Nat. Rev. Endocrinol.* 15:288–298, 2019.
63. Kleinert, M., C. Clemmensen, S. M. Hofmann, M. C. Moore, S. Renner, S. C. Woods, P. Huypens, J. Beckers, M. H. de Angelis, A. Schürmann, M. Bakhti, M. Klingenspor, M. Heiman, A. D. Cherrington, M. Ristow, H. Lickert, E. Wolf, P. J. Havel, T. D. Müller, and M. H. Tschöp. Animal models of obesity and diabetes mellitus. *Nat. Rev. Endocrinol.* 14:140–162, 2018.
64. Suganami, T., J. Nishida, and Y. Ogawa. A paracrine loop between adipocytes and macrophages aggravates inflammatory changes. *Arterioscler. Thromb. Vasc. Biol.* 25:2062–2068, 2005.
65. Khan, T., E. S. Muise, P. Iyengar, Z. V. Wang, M. Chandalia, N. Abate, B. B. Zhang, P. Bonaldo, S. Chua, and P. E. Scherer. Metabolic dysregulation and adipose tissue fibrosis: role of collagen VI. *Mol. Cell. Biol.* 29:1575, 2008.
66. Sun, K., X. Li, and P. E. Scherer. Extracellular matrix (ECM) and fibrosis in adipose tissue: overview and perspectives. *Compr. Physiol.* 13:4387, 2023.

**Publisher's Note** Springer Nature remains neutral with regard to jurisdictional claims in published maps and institutional affiliations.

Springer Nature or its licensor (e.g. a society or other partner) holds exclusive rights to this article under a publishing agreement with the author(s) or other rightsholder(s); author self-archiving of the accepted manuscript version of this article is solely governed by the terms of such publishing agreement and applicable law.

**Supplementary Table 1:** Primer sequences used for quantitative real-time PCR assays.

<b>Gene</b>	<b>Forward Sequence (5' – 3')</b>	<b>Reverse Sequence (5' – 3')</b>
<i>PPARG</i>	CACAAGAACAGATCCAGTGGTTG CAG	AATAATAAGGTGGAGATGCAGGC TCC
<i>FABP4</i>	ACGAGAGGATGATAAACTGGTGG	GCGAACTTCAGTCCAGGTCAAC
<i>ADIPOQ</i>	AACATGCCCATTCGCTTTACC	TAGGCAAAGTAGTACAGCCCA
<i>PLIN1</i>	GACCTCCCTGAGCAGGAGAT	GTGGGCTTCCTTAGTGCTGG
<i>IL6</i>	ACTCACCTCTTCAGAACGAATTG	CCATCTTTGGAAGGTTTCAGGTTG
<i>18S</i>	CGGCGACGACCCATTCGAAC	GAATCGAACCCCTGATTCCCCGTC

**Supplementary Figure 1:** Timelines of drainage studies for (A) **Fig. 2**, (B) **Fig. 3**, (C) **Fig. 5**, and (D) **Fig. 7**. “Day 0” denotes the day on which LECs were seeded into the empty cavities in the gels. Media additives (e.g., insulin) are not listed in the figure and are provided in the Methods section. LM, lymphatic medium; DM, differentiation medium; CM, conditioned medium.

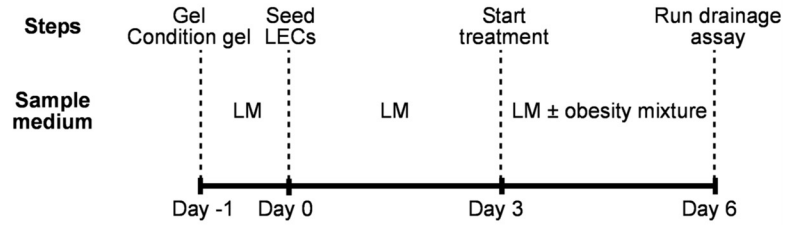
**Supplementary Figure 2:** Elastic moduli of collagen matrices. Data are from three independent experiments. \*\*\*,  $p < 0.001$ ; *n.s.*, not significant.

**Supplementary Figure 3:** Prox1 (*red*) and Hoechst (*blue*) stain of LECs, ASCs after three weeks of adipogenic differentiation, and undifferentiated ASCs in 2D culture.

Supplementary Figure 1:

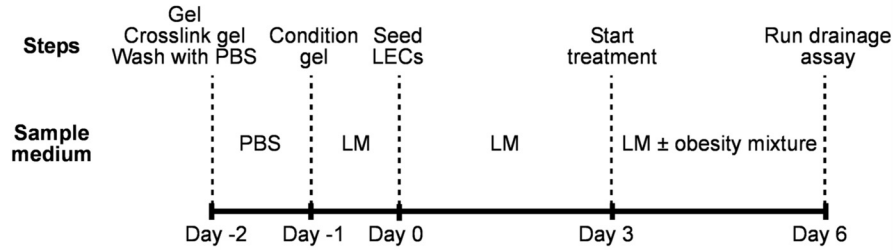
A

Fig. 2 - Uncrosslinked adipocyte-free collagen



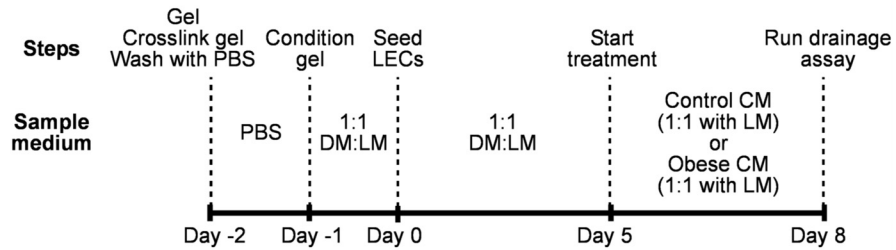
B

Fig. 3 - Crosslinked adipocyte-free collagen



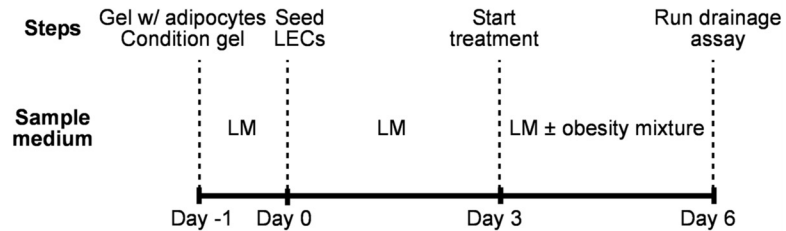
C

Fig. 5 - Crosslinked adipocyte-free collagen with CM

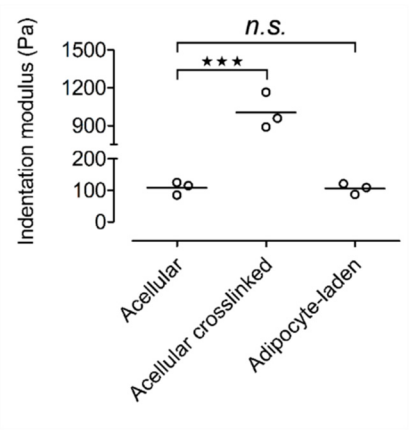


D

Fig. 7 - Uncrosslinked adipocyte-laden collagen



Supplementary Figure 2:



Supplementary Figure 3:

